

Three-Mode Squeezing of Simultaneous and Ordinal Cascaded Four-Wave Mixing Processes in Rubidium Vapor

Wei Li, Changbiao Li, Mengqi Niu, Binshuo Luo, Irfan Ahmed, Yin Cai,*
and Yanpeng Zhang

Multipartite quantum correlation plays a vital role in potential applications of quantum technologies. In this paper, using energy-level cascaded four-wave mixing (EC-FWM) process, a scheme to produce quantum correlated three-mode light beams within a single device of hot atomic medium of rubidium is proposed. Two- and three-mode amplitude, phase quadrature squeezing and intensity difference squeezing using energy-level simultaneous cascaded FWM (ESC-FWM) method and energy-level ordinal cascaded FWM (EOC-FWM) method, respectively, is theoretically reported. Via investigating their covariance matrix properties, the comparison has been made between the two methods, which shows the ESC-FWM method has a more stable mode structure than EOC-FWM method. Moreover, versatile gain dependent squeezing via EC-FWM is studied and analytical expressions are given. These results show a simplified and efficient experimental scheme producing multipartite quantum correlation among multiple spatially separated beams.

1. Introduction

Squeezed and entangled optical fields are essential resources in quantum metrology and quantum information.^[1] In the discrete variable regime, spontaneous parametric down-conversion (SPDC) generates correlated photon.^[2–8] In a continuous-variable regime, four-wave mixing (FWM) process has several strengths compared with SPDC in practical implementation. For example, it does not need a cavity to the system and has strong nonlinearity, spatially separated correlated beams and so on. The parametric amplification FWM (PA-FWM) process produces

narrow-band bright entangled light beams.^[9–14] And the FWM process in the rubidium (Rb) atomic system is one of proven candidates for the generation of correlated twin beams.^[15–24]


Multimode quantum states (MQS) are considered as an essential resource for a fundamental test of quantum physics,^[25–28] and have attracted considerable attention.^[29,30] The reliable methods based on the FWM process for generating MQS have been theoretically proved and experimentally implemented in the different kinds of systems.^[31–37] For example, cascaded FWM processes in two Rb cells has been used to generate triple correlated beams between signal and idler.^[36,37] And using two pump beams of the same frequency to cascade FWM processes to generate multimode quantum correlated beams.^[38–43]

Recently, the dressed fields are employed to enhance the degree of squeezing^[44,45] and generate the MQS based PA-FWM process. Inspired by previous work, in this paper, we propose a different scheme, that is, energy-level cascaded FWM (EC-FWM) process to produce MQS in a single Rb cell. Two pump beams with different frequencies and one probe beam are employed to create two PA-FWM processes. Two generation paths may exist for these two processes, that is, simultaneous generation and ordinal generation. Therefore, we consider energy-level simultaneous cascaded FWM (ESC-FWM) method model and energy-level ordinal cascaded FWM method (EOC-FWM) method model to investigate two- and three-mode amplitude, phase quadrature squeezing and intensity difference squeezing (IDS) of EC-FWM process. In the ESC-FWM (EOC-FWM) method, PA-FWM1 and PA-FWM2 processes occur simultaneously (sequentially). Instead of cascaded FWM processes in the two Rb cells,^[36,37] here we require only a single Rb cell making setup simple with less optical loss thus enhancing squeezing limit.^[36] Our scheme can intrinsically generate three colors entangled triple beams with spatially asymmetric structures.

This paper is constructed as follows. In section 2, EC-FWM process is briefly introduced. In section 3, we use amplitude, phase quadrature squeezing to characterize multimode squeezing existing in this system. Various combinatorial squeezing among the output of the triple beams are deduced and a comparison between these two methods (ESC-FWM and EOC-FWM) has been achieved based on the results. In section 4, IDS is also

W. Li, Prof. C. Li, M. Niu, B. Luo, Prof. Y. Cai, Prof. Y. Zhang[†]
Key Laboratory for Physical Electronics and Devices of the Ministry of
Education & Shaanxi Key Lab of Information Photonic Technique
Xi'an Jiaotong University
Xi'an 710049, China
E-mail: caiyin@xjtu.edu.cn

Dr. I. Ahmed
Department of Physics
City University of Hong Kong
Kowloon, Hong Kong SAR 999077, China
Dr. I. Ahmed
Electrical Engineering Department
Sukkur IBA University
Sindh 65200 Pakistan

 The ORCID identification number(s) for the author(s) of this article can be found under <https://doi.org/10.1002/andp.202100006>

[†]Yin Cai and Yanpeng Zhang are Co-corresponding author.

DOI: 10.1002/andp.202100006

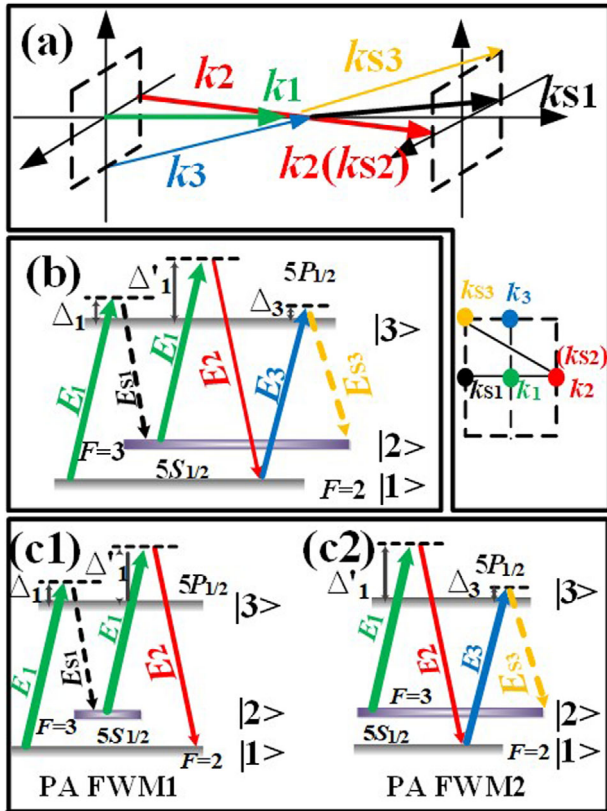


Figure 1. a) Spatial phase matching schematic. b) Energy-level diagram for the three levels configuration in $D1$ line of ^{85}Rb of the EC-FWM process. c) The EC-FWM process can decompose into two PA-FWM processes. (c1) PA-FWM1 process is one of most popular candidates for the generation of quantum correlated twin beams. (c2) Based on PA-FWM1 process, another pump beam E_3 is blue detuned by Δ_3 about 0.7 GHz, converge in the Rb cell, and PA-FWM2 process will generate.

discussed, we investigate the difference between ESC-FWM and EOC-FWM with the influences of G_1 and G_2 . Finally, a brief conclusion is given in section 5.

2. EC-FWM Process

We consider the three-level “double- Λ ” type atomic system in $D1$ line of ^{85}Rb to generate MQS.^[46] The spatial experimental configuration of the scheme is as seen in **Figure 1a**, three beams, that is, two pump beams with different frequencies E_1 , E_3 , and one probe beam E_2 converge in the Rb cell and generate three spatially separated and quantum correlated beams, that is, E_{S1} , E_{S2} , and E_{S3} . The three relevant energy levels are $5S_{1/2}$, $F = 2$ ($|1\rangle$), $5S_{1/2}$, $F = 3$ ($|2\rangle$), and $5P_{1/2}$ ($|3\rangle$) in ^{85}Rb (see **Figure 1b**). The Δ'_1 and Δ_1 are the frequency detuning of the E_1 field from the transitions $|2\rangle \rightarrow |3\rangle$ and $|1\rangle \rightarrow |3\rangle$, respectively. The Δ_3 is frequency detuning of the E_3 field from the transitions $|1\rangle \rightarrow |3\rangle$. In practice, one could employ a 3 cm long rubidium cell at 130 °C, providing an appropriate gain and low background noise to generate quantum correlation and squeezing among the three generated beams.

In this scheme, the three energy levels system contain two cascaded PA-FWMs. First, as seen **Figure 1c**, a strong pump beam

E_1 with more than 100 milliwatts (frequency ω_1 , wave vector k_1 , Rabi frequency G_1 , vertical polarization) is blue detuned by Δ_1 about 1.5 GHz to couple the $D1$ line transition. And a weak beam E_2 with about tens of microwatts (ω_2 , k_2 , G_2 , horizontal polarization) is blue detuned by Δ'_1 about 4.5 GHz to work as a probe field which propagates at E_1 direction with an angle of 0.5° in the horizontal plane as shown in **Figure 1a**. When the phase-matching condition ($k_{S1} + k_{S2} = 2k_1$) are met, the PA-FWM1 process will occur in the system. This process is also one of most used candidates for the generation of quantum correlated twin beams.^[15] Then, another strong pump field E_3 with about tens of milliwatts (ω_3 , k_3 , G_3 , vertical polarization) is blue detuned by Δ_3 about 0.7 GHz to couple the transition $|1\rangle \rightarrow |3\rangle$, which propagates at E_1 direction with an angle of 0.25° in the vertical plane, and generate non-degenerate E_{S3} of PA-FWM2 process as shown in **Figure 1c2**. As one of the two pump beams and the signal beam are shared, these two processes are connected by E_{S2} signal and are thus cascaded together to form EC-FWM process. To cascade PA-FWM1 and PA-FWM2 processes in a single Rb cell, the angle between the two pump beams and the probe beam are crucial, which need be adjusted to satisfy the phase matching conditions of the two PA-FWM processes. In practice, one optimizes the angle via observing the intensities of the three generated beams. Moreover, for measurements, the pump light E_1 and E_3 can be filtered by a polarizing beam splitter, and newly generated E_{S1} , E_{S2} , and E_{S3} signals are spatially separated and can thus be detected by three homodyne detection apparatuses.

However, these two cascaded PA-FWM processes (PA-FWM1: $k_{S1} + k_{S2} = 2k_1$ and PA-FWM2: $k_{S2} + k_{S3} = k_1 + k_3$) may exist two generation paths. i) The probe beam E_2 is seeded into PA-FWM1 and 2 processes simultaneously, so PA-FWM1 and 2 processes occur simultaneously; ii) The probe beam (E_2) is first seeded into PA-FWM1 process. After being amplified, it is seeded into PA-FWM2 process, so PA-FWM1 and 2 processes occur ordinarily. This case is similar with the cascaded FWM process in two Rb cells. In the next section, we theoretically calculate squeezing properties using energy-level simultaneous cascaded four-wave mixing (ESC-FWM) method and energy-level ordinal cascaded FWM (EOC-FWM) method.

Quantum correlated beams, that is, E_{S1} , E_{S2} , and E_{S3} signals, are generated from double cascaded ($\chi_1^{(3)}$ and $\chi_2^{(3)}$ are the corresponding third-order nonlinear susceptibilities) PA-FWM processes, which can be described by their perturbation chains as $\rho_{22}^{(0)} \xrightarrow{\omega_1} \rho_{32}^{(1)} \xrightarrow{\omega_{S2}} \rho_{12}^{(2)} \xrightarrow{\omega_1} \rho_{32(S1)}^{(3)}$ (E_{S1}), $\rho_{11}^{(0)} \xrightarrow{\omega_1} \rho_{31}^{(1)} \xrightarrow{\omega_{S1}} \rho_{21}^{(2)} \xrightarrow{\omega_1} \rho_{31(S2)}^{(3)}$ (E_{S2}), and $\rho_{22}^{(0)} \xrightarrow{\omega_2} \rho_{31(S2)}^{(3)}$ & $\rho_{11}^{(0)} \xrightarrow{\omega_3} \rho_{31}^{(1)} \xrightarrow{\omega_{S3}} \rho_{21}^{(2)} \xrightarrow{\omega_1} \rho_{31(S2)}^{(3)}$ (E_{S3}), respectively. So, the density matrix of E_{S1} , E_{S2} , and E_{S3} signals can be given by

$$\rho_{32(S1)}^{(3)} = iG_1^2 G_{S2} / d_{32} d_{12} d'_{321} \quad (1a)$$

$$\rho_{31(S2)}^{(3)} = iG_1^2 G_{S1} / d_{311} d_{211} d'_{311} + iG_1 G_3 G_{S3} / d_{312} d_{212} d'_{312} \quad (1b)$$

$$\rho_{32(S3)}^{(3)} = iG_1 G_3 G_{S2} / d_{32} d_{12} d'_{322} \quad (1c)$$

where $d_{32} = \Gamma_{32} + i\Delta'_1$, $d_{12} = \Gamma_{12} + i(\Delta'_1 - \Delta_{S2})$, $d'_{321} = \Gamma_{32} + i(\Delta_1 - \Delta_{S2} + \Delta'_1)$, $d_{311} = \Gamma_{31} + i\Delta_1$, $d_{211} = \Gamma_{21} + i(\Delta_1 - \Delta_{S1})$, $d'_{311} = \Gamma_{31} + i(\Delta_1 - \Delta_{S1} + \Delta'_1)$, $d_{312} = \Gamma_{31} + i\Delta_3$, $d_{212} = \Gamma_{21} + i(\Delta_1 - \Delta_{S3})$,

$d'_{312} = \Gamma_{31} + i(\Delta_1 - \Delta_{S3} + \Delta'_1)$, $d'_{322} = \Gamma_{32} + i(\Delta_3 - \Delta_{S2} + \Delta'_1)$ with Δ_{S1} , Δ_{S2} , and Δ_{S3} representing the frequency detuning of the E_{S1} , E_{S2} , and E_{S3} signals, and $\Gamma_{ij} = (\Gamma_i + \Gamma_j)/2$ is the de-coherence rate between $|i\rangle$ and $|j\rangle$, $G_i = m_{ij}E_{ij}/\hbar$, m_{ij} is the dipole momentum. EC-FWM process has the advantages of simple experimental implementation and spatially separated beams. Moreover, as two pump fields are employed within a single Rb cell, EC-FWM process can generate multiple quantum correlated beams with lower loss and more adjustable parameters.

3. Amplitude Quadrature Squeezing and Phase Quadrature Squeezing

3.1. ESC-FWM Method

First, we consider that a probe beam E_2 is seeded into PA-FWM1 and PA-FWM2 processes simultaneously, one can consider this system configuration as ESC-FWM method, whose Hamiltonian can be written in a good approximate as

$$H_I = i\hbar\kappa_1\hat{a}_1^\dagger\hat{a}_2^\dagger + i\hbar\kappa_2\hat{a}_2^\dagger\hat{a}_3^\dagger + \text{H.c.} \quad (2)$$

where \hat{a}_1^\dagger , \hat{a}_2^\dagger , and \hat{a}_3^\dagger represent the photon creation operators of the output modes; $\kappa_1 = -i\varpi_1\chi_1^{(3)}E_1^2/2c$ and $\kappa_2 = -i\varpi_2\chi_2^{(3)}E_1E_3/2c$ are the interaction strengths of the PA-FWM1 and PA-FWM2 processes, respectively, which includes the nonlinear response of the media and governs the expected conversion rate of PA-FWM process; ϖ_i is the central frequency of generated signals; H.c. is Hermitian conjugate.

The boson-creation (-annihilation) operator satisfies the Heisenberg operator of motion in the dipole approximation. Therefore, the dynamic equation of the system can be written:

$$\frac{d\hat{a}_1}{dt} = \kappa_1\hat{a}_2^\dagger, \quad \frac{d\hat{a}_2}{dt} = \kappa_1\hat{a}_1^\dagger + \kappa_2\hat{a}_3^\dagger, \quad \frac{d\hat{a}_3}{dt} = \kappa_2\hat{a}_2^\dagger \quad (3)$$

After the operation of the time evolution equation, the final input-output relation of ESC-FWM method is written by:

$$\hat{a}_{1out} = \frac{a^2 + \sqrt{G}}{1 + a^2}\hat{a}_{1in} + \sqrt{\frac{g}{1 + a^2}}\hat{a}_{2in}^\dagger + \frac{a(\sqrt{G} - 1)}{1 + a^2}\hat{a}_{3in} \quad (4a)$$

$$\hat{a}_{2out} = \sqrt{\frac{g}{1 + a^2}}\hat{a}_{1in}^\dagger + \sqrt{G}\hat{a}_{2in} + a\sqrt{\frac{g}{1 + a^2}}\hat{a}_{3in}^\dagger, \quad (4b)$$

$$\hat{a}_{3out} = \frac{a(\sqrt{G} - 1)}{1 + a^2}\hat{a}_{1in} + a\sqrt{\frac{g}{1 + a^2}}\hat{a}_{2in}^\dagger + \frac{1 + a^2\sqrt{G}}{1 + a^2}\hat{a}_{3in}, \quad (4c)$$

where $a = \kappa_2/\kappa_1$ represents the interaction strength ratio of the PA-FWM1 and PA-FWM2 processes, the a can be controlled by the introduction of a dressing field to regulate the $\chi^{(3)}$ or by the pump power ratio of E_1 and E_3 . $G = \cosh^2(\Omega t)$, $g = \sinh^2(\Omega t)$, G and g are the total intensity gain of ESC-FWM method, and $\Omega = \sqrt{\kappa_1^2 + \kappa_2^2}$. \hat{a}_{2in} is the coherent input, and \hat{a}_{1in} , \hat{a}_{3in} are the vacuum input. \hat{a}_{2out} is the amplified signal beam and \hat{a}_{1out} , \hat{a}_{3out} are

the generated idler beams from ESC-FWM method. On the basis of amplitude quadrature operators $\hat{X} = \hat{a} + \hat{a}^\dagger$ and phase quadrature operators $\hat{P} = i(\hat{a}^\dagger - \hat{a})$, Equations (4a-c) can be rewritten:

$$\begin{pmatrix} \hat{X}_{1out} \\ \hat{X}_{2out} \\ \hat{X}_{3out} \end{pmatrix} = U_X \begin{pmatrix} \hat{X}_{1in} \\ \hat{X}_{2in} \\ \hat{X}_{3in} \end{pmatrix} \quad (5)$$

$$\begin{pmatrix} \hat{P}_{1out} \\ \hat{P}_{2out} \\ \hat{P}_{3out} \end{pmatrix} = U_P \begin{pmatrix} \hat{P}_{1in} \\ \hat{P}_{2in} \\ \hat{P}_{3in} \end{pmatrix} \quad (6)$$

where

$$U_X = \begin{pmatrix} \frac{a^2 + \sqrt{G}}{1 + a^2} & \sqrt{\frac{g}{1 + a^2}} & \frac{a(\sqrt{G} - 1)}{1 + a^2} \\ \sqrt{\frac{g}{1 + a^2}} & \sqrt{G} & a\sqrt{\frac{g}{1 + a^2}} \\ \frac{a(\sqrt{G} - 1)}{1 + a^2} & a\sqrt{\frac{g}{1 + a^2}} & \frac{1 + a^2\sqrt{G}}{1 + a^2} \end{pmatrix}, \quad (7)$$

$$U_P = \begin{pmatrix} \frac{a^2 + \sqrt{G}}{1 + a^2} & -\sqrt{\frac{g}{1 + a^2}} & \frac{a(\sqrt{G} - 1)}{1 + a^2} \\ -\sqrt{\frac{g}{1 + a^2}} & \sqrt{G} & -a\sqrt{\frac{g}{1 + a^2}} \\ \frac{a(\sqrt{G} - 1)}{1 + a^2} & -a\sqrt{\frac{g}{1 + a^2}} & \frac{1 + a^2\sqrt{G}}{1 + a^2} \end{pmatrix}, \quad (8)$$

Obviously, we can realize from Equations (7) and (8) that the system does not couple \hat{X} and \hat{P} quadrature of the fields, which means that there is no related items between the \hat{X} and \hat{P} , and one can treat them independently. Besides, if the input beams are vacuum or coherent states, we can use the covariance matrix to fully express the system because the system's global transformation is symplectic and it retains Gaussian statistics.^[47] So the covariance matrix of ESC-FWM method can be written:

$$C = \begin{pmatrix} C_{XX} & 0 \\ 0 & C_{PP} \end{pmatrix}, \quad (9)$$

where C_{XX} and C_{PP} respectively represent the amplitude and phase quadrature parts of the covariance matrix of the ESC-FWM method. Off-diagonal elements of the covariance matrix are all zero, suggesting \hat{X} and \hat{P} quadrature are not coupled. We define $C_{XX} = \langle \hat{X}_{1out}, \hat{X}_{2out}, \hat{X}_{3out} \rangle^T \langle \hat{X}_{1out}, \hat{X}_{2out}, \hat{X}_{3out} \rangle$ and $C_{PP} = \langle \hat{P}_{1out}, \hat{P}_{2out}, \hat{P}_{3out} \rangle^T \langle \hat{P}_{1out}, \hat{P}_{2out}, \hat{P}_{3out} \rangle$. Because the variances of coherent and vacuum input modes are normalized to one, subsequently we can derive $C_{XX} = U_X \cdot U_X^T$ and $C_{PP} = U_P \cdot U_P^T$. Because the experimental conditions such as the power and angle of the input beam are set up, the a usually barely change in ESC-FWM method, so we set the a to constant 1 in Equations (7) and (8) for

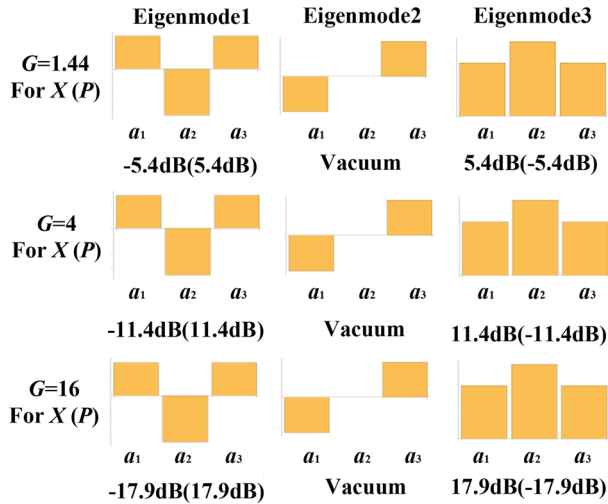


Figure 2. Eigenmodes of the ESC-FWM method, decomposed in the FWM output mode basis, for three different gain values. For each graph, the bars represent the relative weight of modes \hat{a}_{1out} , \hat{a}_{2out} , \hat{a}_{3out} respectively. Below are given the noise variances eigenvalue of the corresponding \hat{X} quadrature and \hat{P} quadrature.

obtaining equal interaction strength of two PA-FWM processes. Finally, we can get:

$$C_{XX} = \begin{pmatrix} G & \sqrt{2Gg} & g \\ \sqrt{2Gg} & G+g & \sqrt{2Gg} \\ g & \sqrt{2Gg} & G \end{pmatrix}, \quad (10)$$

$$C_{PP} = \begin{pmatrix} G & -\sqrt{2Gg} & g \\ -\sqrt{2Gg} & G+g & -\sqrt{2Gg} \\ g & -\sqrt{2Gg} & G \end{pmatrix} \quad (11)$$

The covariance matrix can characterize the relationship between the amplitude and phase quadrature components of the three output modes.^[48] As the system is pure state, we can get the eigenmodes of the system by diagonalizing the covariance matrix, and each eigenmode is a given linear combination of the output modes of ESC-FWM method.

When we set $G = 1.44, 4, \text{ or } 16$, respectively in Equations (10) and (11), we can obtain the corresponding eigenvalues and eigenmodes of C_{XX} and C_{PP} .

As the results in **Figure 2** suggest, for instance when the gain $G = 1.44$, the eigenmodes of C_{XX} are $(0.5, -0.7071, 0.5)$, $(-0.7071, 0, 0.7071)$, $(0.5, 0.7071, 0.5)$, which have been normalized. Corresponding eigenvalues are $0.288, 1.0, 3.47$, and the degree of squeezing of these eigenvalues are $-5.4, 0, 5.4$ dB, respectively, which means that the system is made up of only two squeezed eigenmodes (Eigenmode 1 and 3) and one vacuum eigenmode (Eigenmode 2). Interestingly their relative weight of modes $(\hat{a}_{1out}, \hat{a}_{2out}, \hat{a}_{3out})$ does not change with gain G as shown in **Figure 2**. This shows a stable mode structure in this system, suggested by simultaneous PA-FWM1 and PA-FWM2 processes.

Table 1. Amplitude and phase quadrature squeezing of ESC-FWM method between two output beams when set G to 1.44.

$X(\text{dB})$	$G = 1.44$	$P(\text{dB})$	$G = 1.44$
$\text{Var}(X_2 - X_1)$	-2.72	$\text{Var}(P_2 - P_1)$	4.45
$\text{Var}(X_2 + X_1)$	4.45	$\text{Var}(P_2 + P_1)$	-2.72
$\text{Var}(X_2 - X_3)$	-2.72	$\text{Var}(P_2 - P_3)$	4.45
$\text{Var}(X_2 + X_3)$	4.45	$\text{Var}(P_2 + P_3)$	-2.72
$\text{Var}(X_3 - X_1)$	0	$\text{Var}(P_3 - P_1)$	0
$\text{Var}(X_3 + X_1)$	2.74	$\text{Var}(P_3 + P_1)$	2.74

As shown in **Figure 2**, by comparing this two quadrature, that is, \hat{X} quadrature and \hat{P} quadrature, we can see that they have the same eigenmodes but with inverse eigenvalues, because C_{XX} is merely the inverse of C_{PP} . It should be noted that three eigenmodes are uncorrelated, so any other output mode can consist of these three eigenmodes. Subsequently, we can get the amplitude quadrature squeezing between two output modes and three output modes by combining linearly these three eigenmodes,

$$\text{Var}(X_i - X_j) = \beta^T C_{XX} \beta, \quad (12)$$

where β is the normalized output mode we want to calculate, for example, the β of $\text{Var}(X_2 - X_1)$ is $(-1/\sqrt{2}, 1/\sqrt{2}, 0)^T$. In order to facilitate understanding, the calculations of the entire paper are normalized. For the covariance matrix of C_{XX} , we can always find a unitary transformation σ , makes $C_{XX} = \sigma^T \lambda \sigma$, so the Equation (12) can be derived as:

$$\text{Var}(X_i - X_j) = \beta^T \sigma^T \lambda \sigma \beta, \quad (13)$$

where σ is the eigenmode of C_{XX} , λ is corresponding eigenvalue. So the amplitude quadrature squeezing of $\text{Var}(X_2 - X_1)$ can be calculated as -2.72 dB. Equivalent definition applies for phase quadrature squeezing $\text{Var}(P_1 - P_j)$. we can theoretically measure the two-mode amplitude and phase quadrature squeezing.

As shown in **Table 1**, degree of two-mode amplitude quadrature squeezing $\text{Var}(X_2 - X_1)$ and $\text{Var}(X_2 - X_3)$ is smaller than zero, and interestingly they have the same squeezing values -2.72 dB, showing a good symmetry system. The degree of squeezing corresponding \hat{X} quadrature and \hat{P} quadrature between two conjugate beams $(\hat{a}_{1out}$ and $\hat{a}_{3out})$ is zero as shown in **Table 1**, it shows that there is no squeezing.

Then, we fully consider these eight cases of three-mode amplitude and phase quadrature squeezing. The amplitude quadrature squeezing of $\text{Var}(X_2 - X_1 - X_3)$ is smaller than zero, showing that three-mode squeezing exists. From **Table 2**, the output modes with opposite sign correspond to same mode, so they must have the same squeezing value. For example, the amplitude quadrature squeezing of $\text{Var}(X_2 - X_1 - X_3)$ and $\text{Var}(X_1 + X_3 - X_2)$ is both -4.21 dB. So we can calculate the value of only top four of these cases in **Table 2**, and the rest four can be predicted.

3.2. EOC-FWM Method

Now we consider PA-FWM1 ($k_{S1} + k_{S2} = 2k_1$) process and PA-FWM2 ($k_{S2} + k_{S3} = k_1 + k_3$) process occur sequentially unlike

Table 2. Amplitude and phase quadrature squeezing of ESC-FWM method between three output beams when set G to 1.44.

$X(\text{dB})$	$G = 1.44$	$P(\text{dB})$	$G = 1.44$
$\text{Var}(X_2 - X_1 - X_3)$	-4.21	$\text{Var}(P_2 - P_1 - P_3)$	5.29
$\text{Var}(X_2 + X_1 + X_3)$	5.29	$\text{Var}(P_2 + P_1 + P_3)$	-4.21
$\text{Var}(X_2 - X_1 + X_3)$	1.12	$\text{Var}(P_2 - P_1 + P_3)$	1.12
$\text{Var}(X_2 + X_1 - X_3)$	1.12	$\text{Var}(P_2 + P_1 - P_3)$	1.12
$\text{Var}(X_1 + X_3 - X_2)$	-4.21	$\text{Var}(P_1 + P_3 - P_2)$	5.29
$\text{Var}(-X_2 - X_1 - X_3)$	5.29	$\text{Var}(-P_2 - P_1 - P_3)$	-4.21
$\text{Var}(X_1 - X_2 - X_3)$	1.12	$\text{Var}(P_1 - P_2 - P_3)$	1.12
$\text{Var}(X_3 - X_2 - X_1)$	1.12	$\text{Var}(P_3 - P_2 - P_1)$	1.12

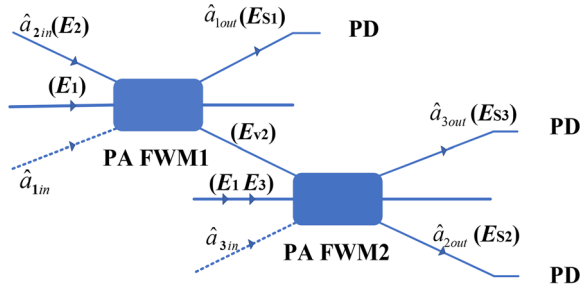


Figure 3. The theory structure diagram for the EOC-FWM method. In the EOC-FWM method, PA-FWM1 and PA-FWM2 processes occur sequentially. E_{s1} is the generated idler beam and E_{v2} is an amplified signal beam from the PA-FWM1 process. E_{s2} is the amplified signal beam and E_{s3} is the generated idler beam from the PA-FWM2 process.

ESC-FWM method. As shown in **Figure 3**, a coherent probe beam (E_2) is seeded into PA-FWM1 process and generate correlated twin beams (E_{s1} and E_{v2}). Amplified E_{v2} beam is then seeded into PA-FWM2 process. Finally, we can obtain three-mode correlated beams (E_{s1} , E_{s2} , and E_{s3}) through two ordinal PA-FWM processes. Since PA-FWM1 and PA-FWM2 processes are not generated simultaneously, so we can express separate Hamiltonian:

$$H_1 = i\hbar\kappa_1\hat{a}_1^\dagger\hat{a}_2^\dagger + \text{H.c.}, \quad (14a)$$

$$H_2 = i\hbar\kappa_2\hat{a}_2^\dagger\hat{a}_3^\dagger + \text{H.c.}, \quad (14b)$$

where $\kappa_1 = -i\omega_1\chi_1^{(3)}E_1^2/2c$ and $\kappa_2 = -i\omega_2\chi_2^{(3)}E_1E_3/2c$ are the same as the definition of ESC-FWM method, but the Hamiltonian of EOC-FWM method is different with ESC-FWM method. The input–output relationship of EOC-FWM method is given by:

$$\hat{a}_{1out} = \sqrt{G_1}\hat{a}_{1in} + \sqrt{g_1}\hat{a}_{2in}^\dagger, \quad (15a)$$

$$\hat{a}_{2out} = \sqrt{g_1G_2}\hat{a}_{1in}^\dagger + \sqrt{G_1G_2}\hat{a}_{2in} + \sqrt{g_2}\hat{a}_{3in}^\dagger, \quad (15b)$$

$$\hat{a}_{3out} = \sqrt{g_1g_2}\hat{a}_{1in} + \sqrt{G_1g_2}\hat{a}_{2in}^\dagger + \sqrt{G_2}\hat{a}_{3in}, \quad (15c)$$

where we define $G_1 = \cosh^2(\kappa_1 t)$, $G_2 = \cosh^2(\kappa_2 t)$ is the intensity gain of the PA-FWM1 and PA-FWM2 processes, respec-

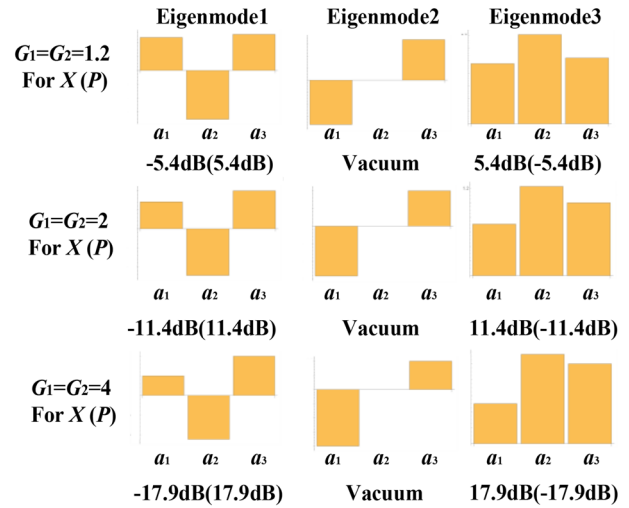


Figure 4. Eigenmodes of the EOC-FWM method, decomposed in the FWM output mode basis, for three different gain values. For each graph, the bars represent the relative weight of modes \hat{a}_{1out} , \hat{a}_{2out} , and \hat{a}_{3out} , respectively. Below are given the noise variances eigenvalue of the corresponding \hat{X} quadrature.

tively and $G_i - g_i = 1$. We can still rewrite the Equation (15a–c) for the \hat{X} quadrature and \hat{P} quadrature, respectively

$$\begin{pmatrix} \hat{X}_{1out} \\ \hat{X}_{2out} \\ \hat{X}_{3out} \end{pmatrix} = \begin{pmatrix} \sqrt{G_1} & \sqrt{g_1} & 0 \\ \sqrt{g_1G_2} & \sqrt{G_1G_2} & \sqrt{g_2} \\ \sqrt{g_1g_2} & \sqrt{G_1g_2} & \sqrt{G_2} \end{pmatrix} \begin{pmatrix} \hat{X}_{1in} \\ \hat{X}_{2in} \\ \hat{X}_{3in} \end{pmatrix}, \quad (16)$$

$$\begin{pmatrix} \hat{P}_{1out} \\ \hat{P}_{2out} \\ \hat{P}_{3out} \end{pmatrix} = \begin{pmatrix} \sqrt{G_1} & -\sqrt{g_1} & 0 \\ -\sqrt{g_1G_2} & \sqrt{G_1G_2} & -\sqrt{g_2} \\ \sqrt{g_1g_2} & -\sqrt{G_1g_2} & \sqrt{G_2} \end{pmatrix} \begin{pmatrix} \hat{P}_{1in} \\ \hat{P}_{2in} \\ \hat{P}_{3in} \end{pmatrix}. \quad (17)$$

Similarly, the covariance matrix of the EOC-FWM method can be obtained by using the same procedure as for Equation (9). It is also block diagonal, and for coherent or vacuum input states each block is given by

$$C_{XX} = \langle U_{X_{3mode}} U_{X_{3mode}}^T \rangle, \quad (18)$$

$$C_{PP} = \langle U_{P_{3mode}} U_{P_{3mode}}^T \rangle, \quad (19)$$

we set $G_1 = G_2$ to 1.2, 2, or 4 to obtain the corresponding eigenvalues and eigenmodes of C_{XX} and C_{PP} as follows

As **Figure 4** suggests, we can see the degree of squeezing of these three eigenvalues is (-5.4, 0, and 5.4 dB) for \hat{X} quadrature when $G_1 = G_2$ set to 1.2, which is same as ESC-FWM (see Figure 2) when G set to 1.44. This shows that their eigenvalues are same when the two methods have the same pump power. Interestingly, this system also consists of two independent squeezed eigenmodes and a vacuum eigenmode, yet with different relative weight of the modes \hat{a}_{1out} , \hat{a}_{2out} , \hat{a}_{3out} compared with the ESC-FWM method. And the relative weight of modes \hat{a}_{1out} , \hat{a}_{2out} , \hat{a}_{3out}

Table 3. Amplitude and phase quadrature squeezing of EOC-FWM method between two and three output beams when set $G_1 = G_2 = 1.2$.

$X(\text{dB})$	$G_1 = G_2 = 1.2$	$P(\text{dB})$	$G_1 = G_2 = 1.2$
two-mode			
$\text{Var}(X_2 - X_1)$	-2.47	$\text{Var}(P_2 - P_1)$	4.34
$\text{Var}(X_2 + X_1)$	4.34	$\text{Var}(P_2 + P_1)$	-2.47
$\text{Var}(X_2 - X_3)$	-2.97	$\text{Var}(P_2 - P_3)$	4.56
$\text{Var}(X_2 + X_3)$	4.56	$\text{Var}(P_2 + P_3)$	-2.97
$\text{Var}(X_3 - X_1)$	0	$\text{Var}(P_3 - P_1)$	0
$\text{Var}(X_3 + X_1)$	2.74	$\text{Var}(P_3 + P_1)$	2.74
three-mode			
$\text{Var}(X_2 - X_1 - X_3)$	-4.21	$\text{Var}(P_2 - P_1 - P_3)$	5.29
$\text{Var}(X_2 + X_1 + X_3)$	5.29	$\text{Var}(P_2 + P_1 + P_3)$	-4.21
$\text{Var}(X_2 - X_1 + X_3)$	1.35	$\text{Var}(P_2 - P_1 + P_3)$	0.89
$\text{Var}(X_2 + X_1 - X_3)$	0.89	$\text{Var}(P_2 + P_1 - P_3)$	1.35
$\text{Var}(X_1 + X_3 - X_2)$	-4.21	$\text{Var}(P_1 + P_3 - P_2)$	5.29
$\text{Var}(-X_2 - X_1 - X_3)$	5.29	$\text{Var}(-P_2 - P_1 - P_3)$	-4.21
$\text{Var}(X_1 - X_2 - X_3)$	1.35	$\text{Var}(P_1 - P_2 - P_3)$	0.89
$\text{Var}(X_3 - X_2 - X_1)$	0.89	$\text{Var}(P_3 - P_2 - P_1)$	1.35

changes with gain G_1 and G_2 as shown in Figure 4, which is different with the ESC-FWM method as shown in Figure 2. This is mainly because PA-FWM1 and PA-FWM2 processes in the ESC-FWM method occur simultaneously, so the whole system has more stable mode structure compared with the non-simultaneous cascaded system.

As the same procedure we did in the Equation (13), we can get the two- and three-mode amplitude and phase quadrature squeezing by combining linearly these eigenmodes.

By comparing Tables 1, 2, and 3, two-mode amplitude quadrature squeezing $\text{Var}(X_2 - X_1)$ of EOC-FWM is -2.47 dB, smaller than -2.97 dB of $\text{Var}(X_2 - X_3)$. But in ESC-FWM, $\text{Var}(X_2 - X_1)$ has same value -2.72 dB with $\text{Var}(X_2 - X_3)$. This is mainly because in the ESC-FWM method, the distribution among the modes \hat{a}_{1out} and \hat{a}_{3out} are same as shown in Figure 2. This results in $\text{Var}(X_2 - X_1)$ and $\text{Var}(X_2 - X_3)$ having the same value in the ESC-FWM method. Three-mode amplitude quadrature squeezing $\text{Var}(X_2 - X_1 - X_3)$ of EOC-FWM is -4.21 dB, same as that in ESC-FWM.

More generally, the ESC-FWM and EOC-FWM methods models have different Hamiltonians, which determine their quantum characters. The Hamiltonian of the ESC-FWM method can be written as $H_1 = i\hbar\kappa_1\hat{a}_1^\dagger\hat{a}_2^\dagger + i\hbar\kappa_2\hat{a}_2^\dagger\hat{a}_3^\dagger + \text{H.c.}$ in Equation (2), which means that these two PA-FWM processes occur simultaneously. Therefore, one can easily get the dynamic equations as: $d\hat{a}_1/dt = \kappa_1\hat{a}_2^\dagger$, $d\hat{a}_2/dt = \kappa_1\hat{a}_1^\dagger + \kappa_2\hat{a}_3^\dagger$, $d\hat{a}_3/dt = \kappa_2\hat{a}_2^\dagger$ given in Equation (3). For the other case, two PA-FWM processes generate sequentially in the EOC-FWM method, which is analogous to cascading two FWM processes in two separate cells. The Hamiltonian of EOC-FWM method can be written in a good approximate as $H_1 = i\hbar\kappa_1\hat{a}_1^\dagger\hat{a}_2^\dagger + \text{H.c.}$, $H_2 = i\hbar\kappa_2\hat{a}_2^\dagger\hat{a}_3^\dagger + \text{H.c.}$ in Equation (14a,b), and the corresponding dynamic equations are: $d\hat{a}_1/dt = \kappa_1\hat{a}_2^\dagger$, $d\hat{a}_2/dt = \kappa_1\hat{a}_1^\dagger$, $d\hat{a}_2/dt = \kappa_2\hat{a}_3^\dagger$, $d\hat{a}_3/dt = \kappa_2\hat{a}_2^\dagger$. These Hamiltonians in the methods models fully determine the quantum states and quantum correlations among the

modes. For instance, via the two methods, although the squeezing levels are close when the total gain is the same, the distribution of the quantum correlations among the modes are different. Also, due to the unique Hamiltonians in these two methods, the eigenmodes exhibit different modes combinations and squeezing levels.

4. Intensity Difference Squeezing

4.1. ESC-FWM Method

Next, compared with the above amplitude and phase quadrature squeezing, IDS can also be used to characterize the multimode correlation existed in the EC-FWM process.

The input-output relationship of energy-level simultaneous ESC-FWM method is given in Equation (4a,c). Subsequently, the two-mode IDS could be written:

$$Sq_{i-j} = 10 \lg \frac{\text{Var}(I_i - I_j)}{\text{Var}(I_i - I_j)_{SNL}}, \quad (20)$$

where photocurrents $I_i = \hat{a}_{iout}^\dagger \hat{a}_{iout}$ and $I_j = \hat{a}_{jout}^\dagger \hat{a}_{jout}$ is the intensity of output beams. $\text{Var}(I_i - I_j)$ is the mean square deviation of the intensity difference between I_i and I_j . $\text{Var}(I_i - I_j)_{SNL}$ is the corresponding shot noise limit (SNL), and it is equal to the sum of the mean value of the output photon number. First, we consider the degree of two-mode IDS.

$$\begin{aligned} \text{Var}(I_2 - I_1) &= \text{Var}(\hat{a}_{2out}^\dagger \hat{a}_{2out} - \hat{a}_{1out}^\dagger \hat{a}_{1out}) \\ &= \frac{[g^4(\sqrt{G}-1)^2 + g^2(a^2\sqrt{G}+1)^2 + (1+a^2)(1+\sqrt{G}a^2)^2]}{(1+a^2)^3} \langle \hat{a}_{2in}^\dagger \hat{a}_{2in} \rangle, \end{aligned} \quad (21)$$

$$\text{Var}(I_2 - I_1)_{SNL} = \left[\frac{g}{(1+a^2)} + G \right] \langle \hat{a}_{2in}^\dagger \hat{a}_{2in} \rangle. \quad (22)$$

So the degree of IDS between \hat{a}_{1out} and \hat{a}_{2out} is given by

$$\begin{aligned} Sq_{2-1} &= 10 \lg \frac{g^4(\sqrt{G}-1)^2 + g^2(a^2\sqrt{G}+1)^2 + (1+a^2)(1+\sqrt{G}a^2)^2}{g(1+a^2)^2 + G(1+a^2)^3}, \end{aligned} \quad (23)$$

Equation (23) can evolve to $Sq_{2-1} = -10 \lg(2G - 1)$ as $\kappa_2 = 0$. The result has been experimentally certified.^[36,44]

Similarly, the other degrees of IDS between \hat{a}_{2out} and \hat{a}_{3out} , \hat{a}_{1out} and \hat{a}_{3out} are given by

$$Sq_{2-3} = 10 \lg \left[\frac{g^2(1-\sqrt{G})^2 + g(\sqrt{G}+a^2)^2}{G(1+a^2)^3 + g^2(1+a^2)^2} + \frac{(1+a^2)(G+a^2)^2}{G(1+a^2)^3 + g^2(1+a^2)^2} \right], \quad (24)$$

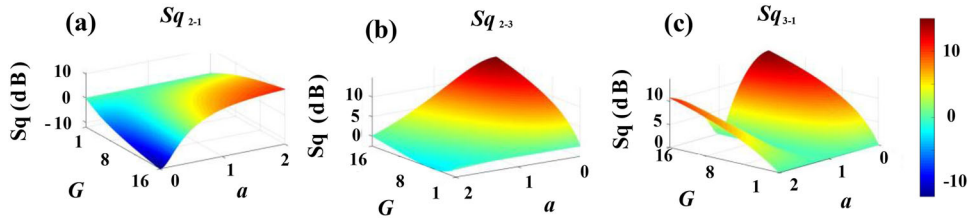


Figure 5. The dependence of two-mode IDS a) Sq_{2-1} b) Sq_{2-3} c) Sq_{3-1} on gain G and a of the ESC-FWM method.

$$Sq_{3-1} = 10 \lg \left[\frac{(1-a^2)^2(1+a^2)g + (2a^2 + \sqrt{G} - a^2\sqrt{G})^2}{(1+a^2)^3} + \frac{(a\sqrt{G} - a^3\sqrt{G} - 2a)^2}{(1+a^2)^3} \right]. \quad (25)$$

When $\kappa_2 = 0$ as field E_3 is off, Equations (24) and (25) degenerate to $Sq_{2-3} = 10 \lg(2G - 1)$ and $Sq_{3-1} = 10 \lg(2G - 1)$, respectively. Normally, the above results are always greater than 0 due to $G > 1$. So, there is no IDS between \hat{a}_{2out} and \hat{a}_{3out} , \hat{a}_{1out} and \hat{a}_{3out} When $\kappa_2 = 0$.

Based on Equations (23–25), **Figure 5** shows the theoretical curves of two-mode IDS versus total gain G ($G = \cosh^2(\sqrt{\kappa_1^2 + \kappa_2^2}t)$) and pump beam power ratio a ($a = \kappa_2/\kappa_1$) in the ESC-FWM. **Figure 5a** shows the variation of two-mode Sq_{2-1} of PA-FWM2 process with G and a . The degree of two-mode Sq_{2-1} increases with the G , but decreases with a . This is mainly because of the definitions of gain G and a . When a increases, κ_1 decreases, and the $G_1 = \cosh^2(\kappa_1 t)$ decreases correspondingly, so the degree of two-mode Sq_{2-1} decreases, as shown in **Figure 5a**. However, when gain G increases and a decreases, so the G_1 increases correspondingly and the degree of Sq_{2-1} increases, which has been experimentally verified.^[44] **Figure 5b** shows the variation of two-mode Sq_{2-3} of PA-FWM2 process with G and a . Obviously, the degree of Sq_{2-3} increases with a . This is mainly because of the increase of a leads to the increase of $G_2 = \cosh^2(\kappa_2 t)$ of PA-FWM2, increasing the degree of IDS of PA-FWM2. **Figure 5c** shows the variation of two-mode Sq_{3-1} between two idle beams versus G and a . When a is equal to 1 which mean that PA-FWM1 and PA-FWM2 processes have the same interaction strength, the value of Sq_{3-1} is always 0, indicate that $Var(I_3 - I_1)$ is equal to $Var(I_3 - I_1)_{SNL}$. But we cannot find that Sq_{3-1} is below zero, this is because that \hat{a}_{1out} and \hat{a}_{3out} do not interact with each other directly.

To verify the effect of G_1 and G_2 on IDS of ESC-FWM method and comprehensively compare with the EOC-FWM method, the total gain G and a in Equations (23–25) are divided into two independent gains $G_1 = \cosh^2(\kappa_1 t)$ and $G_2 = \cosh^2(\kappa_2 t)$, then we set G_1 or G_2 to a certain value 1.2 respectively, and get dependence of Sq_{2-1} , Sq_{2-3} , and Sq_{1-3} on the G_1 (**Figure 6a**) and G_2 (**Figure 6b**). The curve (a1) in **Figure 6a** shows that the degree of Sq_{2-1} changes from anti-squeezing to squeezing as the G_1 increases. This is mainly because a increases with G_1 , therefore, the degree of Sq_{2-1} increase with G_1 . But, the degree of Sq_{2-1} has an opposite tendency as G_2 increases as shown in curve (b1). Similarly, the degree of Sq_{2-3} decreases with G_1 but increases with G_2 , as shown in curve (a2) and (b2). Also, when G_2 increases, the

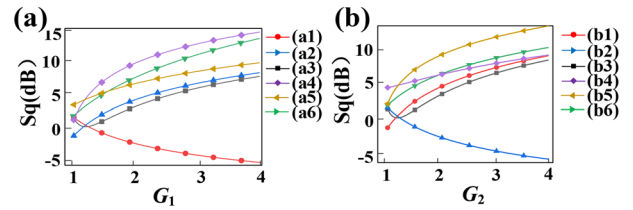


Figure 6. a,b) The dependence of IDS (a1/b1) Sq_{2-1} , (a2/b2) Sq_{2-3} , (a3/b3) Sq_{3-1} and intensity sum squeezing (a4/b4) Sq_{2+1} , (a5/b5) Sq_{2+3} , (a6/b6) Sq_{3+1} on G_1 ($G_2 = 1.2$) and G_2 ($G_1 = 1.2$), respectively, for the ESC-FWM method.

values of the gain G and a in Equation (25) increase, which will cause an increase of the degree of Sq_{3-1} , as shown in curve (b3). And degree of Sq_{3-1} also has an opposite tendency as G_1 increases as shown in curve (a3). Especially, the degrees of intensity sum squeezing Sq_{2+1} , Sq_{2+3} , Sq_{3+1} are all above the zero, and decreases with the G_1 and G_2 , showing there is no IDS at all.

Next, we further study the detailed relation in three-mode IDS, we not only consider the IDS Sq_{2-1-3} , but also we calculate other squeezing cases, that is, intensity sum squeezing Sq_{2+1+3} , and combinatorial squeezing Sq_{2-1+3} and Sq_{2+1-3} . First, we calculate the degree of Sq_{2-1-3} , the mean square deviation of the intensity difference between the three outputs is:

$$\begin{aligned} Var(I_2 - I_1 - I_3) &= Var(\hat{a}_{2out}^\dagger \hat{a}_{2out} - \hat{a}_{1out}^\dagger \hat{a}_{1out} - \hat{a}_{3out}^\dagger \hat{a}_{3out}) = \langle \hat{a}_{2in}^\dagger \hat{a}_{2in} \rangle, \end{aligned} \quad (26)$$

and corresponding SNL is the sum of photon numbers of three coherent laser beams.

$$Var(I_2 - I_1 - I_3)_{SNL} = (2G - 1) \langle \hat{a}_{2in}^\dagger \hat{a}_{2in} \rangle, \quad (27)$$

so, the degree of Sq_{2-1-3} is given by

$$Sq_{2-1-3} = 10 \lg \frac{1}{(2G - 1)}, \quad (28)$$

Similarly, the other degrees of three-mode IDS are given by

$$Sq_{2+1+3} = \lg \frac{(2G - 1)^2 + 4G(G - 1)}{(2G - 1)}, \quad (29)$$

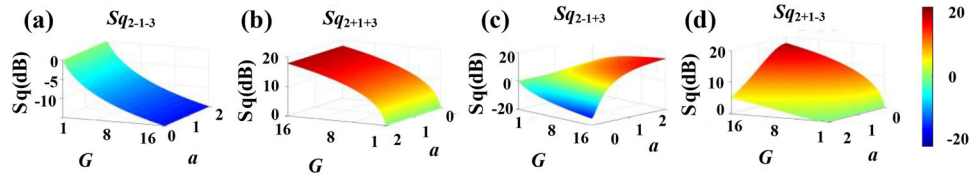


Figure 7. The dependence of three-mode IDS a) Sq_{2-1-3} , b) Sq_{2+1+3} , c) Sq_{2-1+3} , and d) Sq_{2+1-3} on G and a of ESC-FWM method.

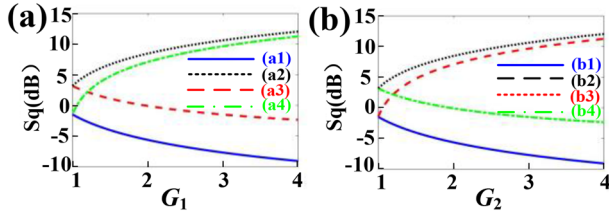


Figure 8. a,b) The dependence of IDS (a1/b1) Sq_{2-1-3} , (a2/b2) Sq_{2+1+3} , (a3/b3) Sq_{2-1+3} and (a4/b4) Sq_{2+1-3} on G_1 ($G_2 = 1.2$) and G_2 ($G_1 = 1.2$), respectively, for the ESC-FWM method.

$$Sq_{2-1+3} = 10 \lg \left[\frac{4a^2(G-1)[a^2(\sqrt{G}-1)^2 + (a^2\sqrt{G}+1)^2]}{(2G-1)(1+a^2)^3} + \frac{(2a^2G-a^2+1)^2(1+a^2)}{(2G-1)(1+a^2)^3} \right], \quad (30)$$

$$Sq_{2+1-3} = 10 \lg \left[\frac{4(G-1)[(a^2+\sqrt{G})^2 + a^2(\sqrt{G}-1)^2]}{(2G-1)(1+a^2)^3} + \frac{(2G+a^2-1)^2(1+a^2)}{(2G-1)(1+a^2)^3} \right]. \quad (31)$$

Subsequently, we can plot the squeezing level from Equations (28–31) in decibels as a function of G and a in **Figure 7**. The result of Sq_{2-1-3} is shown in **Figure 7a** suggesting that there is always three-mode IDS, and the squeezing degree increases with the G , but not change with a , which means that the degree of Sq_{2-1-3} depends only on the total pump power and is independent of the proportional distribution between E_1 and E_3 . As the **Figure 7b** shows, the squeezing degree of intensity sum is always larger than zero, suggesting that there is always no squeezing. **Figure 7c** shows the variation of combinatorial squeezing Sq_{2-1+3} with G and a . The degree of Sq_{2-1+3} increases with G , but decreases with a , this is because when G increases and a decreases, the κ_1 increases faster than κ_2 , and the gain G_1 increases faster than G_2 correspondingly, so the degree of Sq_{2-1+3} increases. **Figure 7d** shows that the degree of Sq_{2+1-3} increases with a , but decrease with G , which is the opposite compared with Sq_{2-1+3} , this is mainly because G_1 and G_2 play different effect to Sq_{2-1+3} and Sq_{2+1-3} , respectively. The effects of G_1 and G_2 in more detail are given below.

Similar with **Figure 6**, we plot the squeezing level as a function of the gain G_1 (**Figure 8a**) and G_2 (**Figure 8b**) by setting G_2 and G_1 to a certain value of 1.2, respectively. As curves (a1) and (b1) in **Figure 8** show, when G_1 and G_2 increase (curves (a2) and (b2) in **Figure 8**), the G in Equation (28) increases, leading to an increase

Table 4. The values of IDS corresponding to Sq_{2-1-3} , Sq_{2+1+3} , Sq_{2-1+3} , Sq_{2+1-3} , respectively when $G_1 = G_2 = 1.2$ for ESC-FWM method.

Sq (dB)	$G_1 = G_2 = 1.2$	Sq (dB)	$G_1 = G_2 = 1.2$
$l_2-l_1-l_3$	-2.67	$l_1+l_3-l_2$	-2.67
$l_2+l_1+l_3$	4.99	$-l_2-l_1-l_3$	4.99
$l_2-l_1+l_3$	2.18	$l_1-l_2-l_3$	2.18
$l_2+l_1-l_3$	2.19	$l_3-l_1-l_2$	2.19

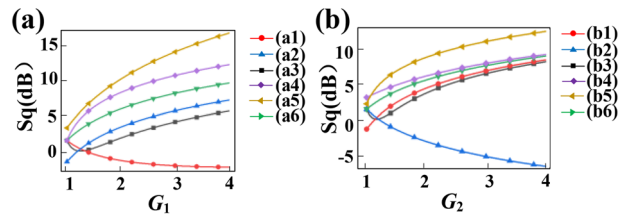


Figure 9. a,b) The dependence of IDS (a1/b1) Sq_{2-1} , (a2/b2) Sq_{2-3} , (a3/b3) Sq_{3-1} and intensity sum squeezing (a4/b4) Sq_{2+1} , (a5/b5) Sq_{2+3} , (a6/b6) Sq_{3+1} on G_1 ($G_2 = 1.2$) and G_2 ($G_1 = 1.2$), respectively, for the EOC-FWM method.

of the degree of Sq_{2-1-3} . Sq_{2+1+3} has opposite trend change as G_1 and G_2 increase (curves (a2) and (b2) in **Figure 8**). From curves (a3) and (b3) in **Figure 8**, the degree of Sq_{2-1+3} increases with G_1 but decreases with G_2 . In fact, PA-FWM1 process promotes the degree of Sq_{2-1+3} but PA-FWM2 process suppresses. As shown in curves (a4) and (b4), Sq_{2+1-3} has opposite trend change as G_1 and G_2 increases compared with Sq_{2-1+3} . Sq_{2-1+3} and Sq_{2+1-3} can never have IDS at the same time, this can be applied potentially to quantum information encryption.

Then we consider the relationship between IDS and amplitude, phase quadrature squeezing of the ESC-FWM method. We can see from **Table 4** that the output mode with opposite sign has the same IDS value. This is same with amplitude and phase quadrature squeezing from **Table 2**. From the left column in **Table 4**, the values of Sq_{2-1-3} , Sq_{2+1+3} , Sq_{2-1+3} , and Sq_{2+1-3} are -2.67, 4.99, 2.18, and 2.19 dB, respectively, and they are different with -4.21, 5.29, 1.12, and 1.12 dB in amplitude and phase quadrature squeezing as shown in **Table 2** under the same gain condition. Because IDS is considered as intensity difference between outputs, and the relative weight of different outputs correspond to their normalized power ratio. But in amplitude and phase quadrature squeezing, the relative weight of outputs is all normalized to equal to 1, which makes the difference between IDS and amplitude and phase quadrature squeezing. In fact, both of IDS and amplitude and phase quadrature squeezing can represent the squeezing properties of the system, and IDS is more convenient to be measured on the experiment.

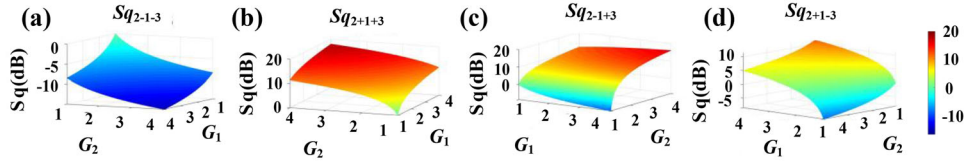


Figure 10. The dependence of three-mode IDS (a) Sq_{2-1-3} , (b) Sq_{2+1+3} , (c) Sq_{2-1+3} , (d) Sq_{2+1-3} , on G_1 and G_2 of EOC-FWM method.

4.2. EOC-FWM Method

Further, we compare IDS between the case of EOC-FWM method and ESC-FWM method. As PA-FWM1 and PA-FWM2 processes occur ordinarily, the Hamiltonian is approximately equivalent to cascaded FWM processed in two separate cells. The expression forms of the degree of two-mode IDS (Sq'_{2-1} , Sq'_{3-1} , and Sq'_{2-3}) are consistent with Ref. [37]. In practice, the intensity gain G_2 ($\propto \kappa_2 \propto \rho_{S2/S3}^{(3)}$) depends on the two pump fields E_1 and E_3 . The reason why there is a slight difference between the ESC-FWM method and the EOC-FWM method is that the cascading paths are different, whose Hamiltonians are given by Equations (2) and (14).

To compare with the case of the ESC-FWM method and EOC-FWM method, we also fix the gain of one of them respectively to a certain value, and obtain the dependence of the degree of IDS with G_1 (Figure 9a) and G_2 (Figure 9b). The results are similar with that in ESC-FWM method as shown in Figure 6.

Then we investigate three-mode IDS. Using the same calculation procedure as in Equations (28–31), the following equation can be obtained

$$Sq'_{2-1-3} = 10 \lg \frac{1}{2G_1 G_2 - 1}, \quad (32)$$

$$Sq'_{2+1+3} = 10 \lg \frac{(2G_1 G_2 - 1)^2 + 4G_1 g_1 G_2^2 + 4G_1 G_2 g_2}{2G_1 G_2 - 1}, \quad (33)$$

$$Sq'_{2-1+3} = 10 \lg \frac{(G_1 G_2 + G_1 g_2 - g_1)^2 + 4G_1 g_1 g_2^2 + 4G_1 G_2 g_2}{2G_1 G_2 - 1}, \quad (34)$$

$$Sq'_{2+1-3} = 10 \lg \frac{(G_1 + g_1)^2 + 4G_1 g_1}{2G_1 G_2 - 1}, \quad (35)$$

We plot the squeezing level from Equations (32–35) in decibels as a function of the G_1 , G_2 as shown in Figure 10. As shown in Figure 10a,b,d, the degrees of Sq'_{2-1-3} , Sq'_{2+1+3} , and Sq'_{2+1-3} are similar with that in ESC-FWM method as shown in Figure 7a,b,d. It can be seen in Figure 10c, Sq'_{2-1+3} of EOC-FWM method has smaller degree of IDS compared with the ESC-FWM method (Figure 7c).

Under the same pump power condition as the ESC-FWM method (see Figure 8), we can clearly see that Sq'_{2-1-3} , Sq'_{2+1+3} , and Sq'_{2+1-3} have the similar results in Figure 11. Sq'_{2-1+3} has no IDS when G_2 set 1.2 as shown in the curve (a3) in Figure 11a3. This further confirms, through EOC-FWM method, the squeezing level of Sq'_{2-1+3} is less than that the ESC-FWM method. This is mainly because compared with the EOC-FWM method, the power ratio between different outputs in Sq_{2-1+3} in the ESC-FWM

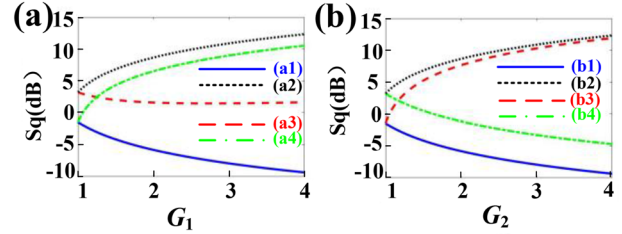


Figure 11. a,b) The dependence of IDS (a1/b1) Sq_{2-1-3} , (a2/b2) Sq_{2+1+3} , (a3/b3) Sq_{2-1+3} and (a4/b4) Sq_{2+1-3} on G_1 ($G_2 = 1.2$) and G_2 ($G_1 = 1.2$), respectively, for the EOC-FWM method.

Table 5. The values of IDS corresponding to Sq_{2-1-3} , Sq_{2+1+3} , Sq_{2-1+3} , and Sq_{2+1-3} respectively when $G_1 = G_2 = 1.2$ for EOC-FWM method.

Sq (dB)	$G_1 = G_2 = 1.2$	Sq (dB)	$G_1 = G_2 = 1.2$
$l_2-l_1-l_3$	-2.74	$l_1+l_3-l_2$	-2.74
$l_2+l_1+l_3$	5.09	$-l_2-l_1-l_3$	5.09
$l_2-l_1+l_3$	2.55	$l_1-l_2-l_3$	2.55
$l_2+l_1-l_3$	1.91	$l_3-l_1-l_2$	1.91

method is closer to the corresponding optimal squeezing eigenmode (see Eigenmode1 in Figures 2 and 4, respectively).

Then we also consider the relationship between IDS and amplitude, phase quadrature squeezing of the EOC-FWM method. Similar with ESC-FWM method in Table 4, we can see that the output mode with opposite sign have the same IDS value from the left and right column in Table 5, this is also same with the case of amplitude, phase quadrature squeezing from Table 3. From the left column in Table 5, the values of Sq'_{2-1-3} , Sq'_{2+1+3} , Sq'_{2-1+3} and Sq'_{2+1-3} are -2.74, 5.09, 2.55, and 1.91 dB respectively, which are similar with amplitude quadrature squeezing, -4.21, 5.29, 1.35, and 0.89 dB, under the same gain condition from Table 3. In fact, both of IDS and amplitude and phase quadrature squeezing can represent the squeezing properties of the system.

5. Conclusion and Discussion

In conclusion, EC-FWM process is proposed to generate three-mode squeezing in a single Rb cell, and we use two different methods (ESC-FWM method and EOC-FWM method) to theoretically investigate their squeezing and quantum correlations. The three-mode squeezing can be efficiently produced and modulated via both methods. The eigenvalues and eigenmodes of the covariance matrix of the two methods are studied. We find, in both methods, it always consists of two independent squeezed eigenmodes and a vacuum eigenmode, and also the squeezing levels

are close when employing same pump powers. Interestingly, the eigenmodes structures of ESC-FWM method do not change with modulating total gain G . This indicates the ratio of the interaction strength in the two PA-FWM processes is constant, and thus ESC-FWM method has a more stable mode structure than EOC-FWM method. Besides, analytical expressions and detailed results of versatile squeezing are given and analyzed. As the Hamiltonians determine the quantum states, the two methods exhibit different squeezing results and quantum properties. Our work, tightly connected to experiments, proposes a new asymmetric scheme to produce three-mode squeezing based on EC-FWM process in a single Rb cell. This scheme could achieve further spatial expansion to realize four or more modes squeezing and entanglement in a single device, and we could use the asymmetric mechanism to actively control the number of mode outputs and the quantum correlations among the modes without using any beam splitters. And by considering its own dressed effect or introducing additional dressed field, it is possible to further precisely control squeezing and entanglement in this scheme.^[44–45]

Acknowledgements

This work was supported by the National Key R&D Program of China (2017YFA0303700, 2018YFA0307500), and National Natural Science Foundation of China (61975159, 61605154, 11604256, 11804267, 11904279).

Conflict of Interest

The authors declare no conflict of interest.

Data Availability Statement

Research data are not shared.

Keywords

amplitude, energy-level cascaded four-wave mixing, intensity difference squeezing, phase quadrature squeezing, three-mode squeezing

Received: January 5, 2021
Revised: February 7, 2021
Published online: March 9, 2021

- [1] N. J. Cerf, G. Leuchs, *Quantum Information with Continuous Variables of Atoms and Light*, Imperial College Press, London **2007**.
- [2] A. Heidmann, R. J. Horowitz, S. Reynaud, E. Giacobino, C. Fabre, G. Camy, *Phys. Rev. Lett.* **1987**, *59*, 2555.
- [3] P. H. Ribeiro, C. Schwob, A. Maître, C. Fabre, *Opt. Lett.* **1997**, *22*, 1893.
- [4] K. S. Zhang, T. Coudreau, M. Martinelli, A. Maître, C. Fabre, *Phys. Rev. A* **2001**, *64*, 033815.
- [5] P. G. Kwiat, K. Mattle, H. Weinfurter, A. Zeilinger, A. V. Sergienko, Y. H. Shih, *Phys. Rev. Lett.* **1995**, *75*, 4337.
- [6] H. Hübel, D. R. Hamel, A. Fedrizzi, S. Ramelow, K. J. Resch, T. Jennewein, *Nature* **2010**, *466*, 601.
- [7] L. K. Shalm, D. R. Hamel, Z. Yan, C. Simon, K. J. Resch, T. Jennewein, *Nat. Phys.* **2013**, *9*, 19.
- [8] G. B. Lemos, V. Borish, G. D. Cole, S. Ramelow, R. Lapkiewicz, A. Zeilinger, *Nature* **2014**, *512*, 409.
- [9] Z. Y. Zhang, F. Wen, J. L. Che, D. Zhang, C. B. Li, Y. P. Zhang, *Sci. Rep.* **2015**, *5*, 15058.
- [10] K. K. Li, R. Bu, D. Zhang, X. H. Li, M. Y. Wen, T. H. Nan, Y. P. Zhang, *Opt. Express* **2017**, *25*, 23556.
- [11] L. Cheng, D. Zhang, J. L. Che, I. Ahmed, H. J. Tang, Z. Y. Zhang, Y. P. Zhang, *Laser Phys.* **2018**, *28*, 095401.
- [12] C. B. Li, B. L. Gu, D. Zhang, W. J. Chen, Z. Shen, G. C. Lan, Y. P. Zhang, *Laser Phys. Lett.* **2019**, *16*, 055401.
- [13] X. H. Xing, Z. D. M. Sun, K. K. Li, Z. G. Wang, Y. P. Zhang, *Europhys. Lett.* **2018**, *122*, 14005.
- [14] C. F. McCormick, V. Boyer, E. Arimonda, P. D. Lett, *Opt. Lett.* **2007**, *32*, 178.
- [15] V. Boyer, A. M. Marino, R. C. Pooser, P. D. Lett, *Science* **2008**, *321*, 544.
- [16] A. M. Marino, R. C. Pooser, V. Boyer, P. D. Lett, *Nature* **2009**, *457*, 859.
- [17] A. I. Lvovsky, M. G. Raymer, *Rev. Mod. Phys.* **2009**, *81*, 299.
- [18] M. Napolitano, M. Koschorreck, B. Dubost, N. Behbood, R. J. Sewell, M. W. Mitchell, *Nature* **2011**, *471*, 486.
- [19] F. Hudelist, J. Kong, C. Liu, J. Jing, Z. Y. Ou, W. Zhang, *Nat. Commun.* **2014**, *5*, 3049.
- [20] R. C. Pooser, B. J. Lawrie, *ACS Photonics* **2016**, *3*, 8.
- [21] B. J. Lawrie, P. G. Evans, R. C. Pooser, *Phys. Rev. Lett.* **2013**, *110*, 156802.
- [22] U. Vogl, R. T. Glasser, J. B. Clark, Q. Glorieux, T. Li, N. V. Corzo, P. D. Lett, *New J. Phys.* **2014**, *16*, 013011.
- [23] Q. Glorieux, L. Guidoni, S. Guibal, J.-P. Likforman, T. Coudreau, *Phys. Rev. A* **2011**, *84*, 053826.
- [24] S. Liu, Y. Lou, J. Jing, *Phys. Rev. Lett.* **2019**, *123*, 113602.
- [25] N. Treps, U. Andersen, B. Buchler, P. K. Lam, A. Maitre, H.-A. Bachor, C. Fabre, *Phys. Rev. Lett.* **2002**, *88*, 203601.
- [26] G. J. de Valcarcel, G. Patera, N. Treps, C. Fabre, *Phys. Rev. A* **2006**, *74*, 061801.
- [27] B. Chalopin, F. Scazza, C. Fabre, N. Treps, *Phys. Rev. A* **2010**, *81*, 061804.
- [28] J. D. Swaim, E. M. Knutson, O. Danaci, R. T. Glasser, *Opt. Lett.* **2018**, *43*, 2716.
- [29] M. Lassen, V. Delaubert, J. Janousek, H. A. B. K. Wagner, P. K. Lam, N. Treps, P. Buchhave, C. Fabre, C. C. Harb, *Phys. Rev. Lett.* **2007**, *98*, 083602.
- [30] D. M. Greenberger, M. A. Horne, A. Zeilinger, *Phys. Today* **1993**, *46*, 22.
- [31] P. van Loock, S. L. Braunstein, *Phys. Rev. Lett.* **2000**, *84*, 3482.
- [32] T. Aoki, N. Takei, H. Yonezawa, K. Wakui, T. Hiraoka, A. Furusawa, P. van Loock, *Phys. Rev. Lett.* **2003**, *91*, 080404.
- [33] H. Yonezawa, T. Aoki, A. Furusawa, *Nature* **2004**, *431*, 430.
- [34] X. Jia, Z. Yan, Z. Duan, X. Su, H. Wang, C. Xie, K. Peng, *Phys. Rev. Lett.* **2012**, *109*, 253604.
- [35] H. Wang, C. Fabre, J. Jing, *Phys. Rev. A* **2017**, *95*, 051802.
- [36] Z. Qin, L. Cao, H. Wang, A. M. Marino, W. Zhang, J. Jing, *Phys. Rev. Lett.* **2014**, *113*, 023602.
- [37] W. Wang, L. M. Cao, Y. B. Lou, J. J. Du, J. T. Jing, *Appl. Phys. Lett.* **2018**, *112*, 034101.
- [38] E. M. Knutson, J. D. Swaim, S. Wyllie, R. T. Glasser, *Phys. Rev. A* **2018**, *98*, 013828.
- [39] S. Liu, H. Wang, J. Jing, *Phys. Rev. A* **2018**, *97*, 043846.
- [40] S. Liu, Y. Lou, J. Jing, *Opt. Express* **2019**, *27*, 37999.
- [41] K. Zhang, W. Wang, S. S. Liu, X. Z. Pan, J. J. Du, Y. B. Lou, S. Yu, S. C. Lv, N. Treps, C. Fabre, J. T. Jing, *Phys. Rev. Lett.* **2020**, *124*, 090501.
- [42] W. Wang, K. Zhang, J. T. Jing, *Phys. Rev. Lett.* **2020**, *125*, 140501.

- [43] Y. Cai, L. Hao, D. Zhang, Y. Liu, B. S. Luo, Z. Zheng, F. Li, Z. Y. Zhang, *Opt. Express* **2020**, *28*, 25278.
- [44] D. Zhang, C. B. Li, Z. Y. Zhang, Y. Q. Zhang, Y. P. Zhang, *Phys. Rev. A* **2017**, *96*, 043847.
- [45] C. B. Li, W. Li, D. Zhang, Z. Y. Zhang, B. L. Gu, K. K. Li, Y. P. Zhang, *Laser Phys. Lett.* **2020**, *17*, 015401.
- [46] R. C. Pooser, A. M. Marino, V. Boyer, K. M. Jones, P. D. Lett, *Opt. Express* **2009**, *19*, 16722.
- [47] Y. Cai, J. L. Feng, H. L. Wang, G. Ferrini, X. Y. Xu, J. T. J., N. Treps, *Phys. Rev. A* **2015**, *91*, 013843.
- [48] S. L. Braunstein, P. van Loock, *Rev. Mod. Phys.* **2005**, *77*, 513.